

# Instrument Flexure & Mechanism Repeatability

## Spartan IR Camera for the SOAR Telescope

Dustin I. Baker & Edwin D. Loh

Department of Physics & Astronomy  
Michigan State University, East Lansing, MI 48824

Loh@msu.edu 517 355-9200 x2480

1 January 2006

### Abstract

We measured the flexure of the instrument and repeatability of the mechanisms at room temperature. Specifically, we measured the movement of the image of a pinhole placed on the field mask, which is at the telescope image surface. The measurement is sensitive to flexure of the optics, mechanisms, and the cryogenic optical box (COB), which supports all; it is insensitive to flexure of the vacuum enclosure and the struts between the vacuum enclosure and COB. The image shift is a sinusoidal function of the orientation of the instrument. The amplitude is  $(-0.16 \pm 0.01, 1.76 \pm 0.03)$  pixels for f/12 and  $(0.01 \pm 0.01, -2.67 \pm 0.07)$  pixels for f/21. (The first number of a pair is the direction for which the instrument is symmetrical.) The residual of the fit is  $(0.03, 0.10)$  pixels for f/12 and  $(0.03, 0.15)$  pixels for f/21, which corresponds to  $(3, 8)$  mas for f/12 and  $(1, 6)$  mas for f/21 in the sky.

On the telescope, flexure can be measured and corrected, if the flexure is reproducible. The residual of the the image shift corrected by the fit of data taken a week earlier is  $(0.06, 0.15)$  pixels, which corresponds to  $(4, 12)$  mas in the sky. Thus the uncorrectable flexure is 0.15 of the diffraction width at a wavelength of 1600 nm.

The mechanisms for the f/12 camera, f/21 collimator, mask, and 2-eye reposition with an RMS shift of  $(0.5, 1.7)$ ,  $(0.7, 3.7)$ ,  $(0.02, 0.13)$ , and  $(0.01, 0.01)$  pixel, respectively, where the shift in the direction of symmetry is the first number of a pair. Therefore, the mask wheel repositions to 0.06 of the diffraction width, and when changing angular resolution, the mechanisms reposition to 1–2 times the diffraction width.

For the flexure test, where the bearing balls do not move in the bearing race, the unreproducible movement of the balls is 10–60 nm. For the test of repeatability of positioning the mechanisms, where the balls do move in the bearing race, the unreproducible movement of the balls is greater by a factor of 30.

# 1 Introduction

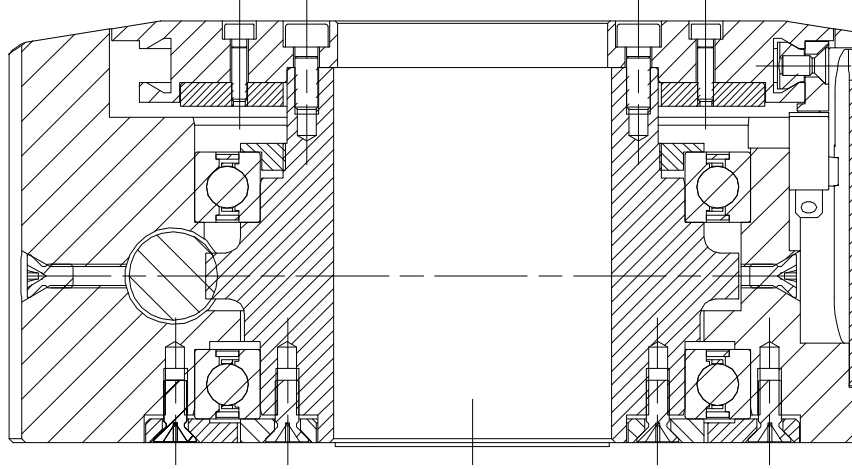


Figure 1: Section view of the PRS110 rotation stage (Private communication, Micos, 2004), which contains a pair of angular contact bearings. The contact between the balls and race of a bearing forms a cone  $40^\circ$  from the axis.

The several mechanism in the Spartan Camera all use PRS110 rotation stages made by Phytron ([www.phytron.com](http://www.phytron.com)) of Waltham, MA, and Micos ([www.micos.ws](http://www.micos.ws)) of Eschbach, Germany. This rotation stage has a pair of angular-contact bearings (Figure 1). Of all the parts in the instrument, the rotation stages are most likely to cause flexure, since the ball bearings are the weakest connections. The loads on the rotation stages are balanced with counterweights.

The instrument is symmetric about the mid-plane of the instrument that is perpendicular to the rotation axis of the telescope. The optics are all on the plane of symmetry.

The first test is to measure the flexure of the instrument as the direction of gravity changes. Mounted at the Nasmyth position, the Spartan Camera turns about one axis as the telescope tracks a star. For the flexure test, a pinhole on the mask, which is at the focus of the telescope, is illuminated by a laser and imaged on the detector. The flexure test does not reveal flexure of the vacuum enclosure and the A-struts, because the shift between the pinhole and the outside is not measured. The calculated shift due to the A-struts is has an amplitude of  $9\,\mu\text{m}$ , which is 30 mas in the sky.

The second test measures the repeatability of the mechanisms. Repeatability of the mask wheel affects operation: For observations with a field mask such as a

coronagraphic mask or a slit, one wants to take a picture without the mask and then insert the mask accurately without the need for additional positioning. Whether the other mechanisms repeat well is not important. If the star moves after changing from the wide-field to the high resolution mode does not affect operation.

A 630-nm laser illuminates a pinhole, which is placed on the mask plate. A multiplexer, the silicon circuit without the HgCdTe sensing layer, is used as a detector to enable operation at room temperature.

In order to measure shifts that are smaller than a pixel, the pinhole is placed far out of focus. The image diameter is 5 pixels. We were not able to measure small shifts with an in-focus image, apparently because the sensitivity of the multiplexer is not uniform across a pixel.

The flexure test jig<sup>1</sup> (Figure 2) supports the entire instrument on an axle, which allows the instrument to rotate 360°. The hoist holds the instrument at a third point.

## 2 Flexure

We measured the shift of the image of the pinhole (Figure 3) as a function of the orientation angle  $\theta$  of the instrument.

The instrument is symmetrical in the direction normal to the large plates of the cryo-optical box. If the symmetry were perfect, the shift in the direction of symmetry should be zero. The shift is indeed small in the direction of symmetry. For the f/12 collimator and f/21 camera mirrors, the symmetry is perfect, and these mirrors cannot shift the image in the direction of symmetry. For the f/12 camera and f/21 collimator, the mechanisms are balanced in the symmetry direction by design and closely but not perfectly balanced in the other direction. Of course, imperfections in the bearings will break the symmetry.

The shifts  $d(\theta)$  are fitted to  $d(\theta) = A \cos(\theta + \phi) + B$ , and the results are in Table 1. The amplitude is about 2 pixels in the non-symmetrical direction and about 0.1 pixel in the symmetrical direction.

Each data set was taken over more than one day, and we discovered a shift in



Figure 2: Spartan Camera in the flexure test jig with orientation  $\theta = +130^\circ$ .

<sup>1</sup>Loh, M., & Loh, E., 2005, “Using the Flexure Test Jig.”

the image position from one day to the next. The residuals in the second column of Figure 3 show the shift. The shift is largest for the f/21 run, which was taken on a Friday and the following Monday. The other two sets were taken on successive days. The fits in the first column of Figure 3 and in Table 1 have the shifts removed.

The phase  $\phi = -11^\circ$  for the f/12 channel and  $45^\circ$  for the f/21 channel, may indicate that the loads on the rotation stages are unbalanced.

The residual from the fit is 0.03–0.15 pixel and 1–8 mas in the sky (Table 1). The diffraction width at  $\lambda 1600$  nm is 80 mas.

If the entire residual is caused by problems in the rotation stages, the residual translates to a tilt of 0.3–1.6  $\mu$ rad at the rotation stages. This is better than the upper limit of our direct measurements made with a coordinate-measuring machine.<sup>2</sup>

Imperfect repeatability flexure are probably due to the bearings in the rotation stages. The PRS110 rotation stage has a pair of angular-contact bearings (Figure 1), and  $R$ , the distance between one bearing and the center of curvature of the other, is 37 mm. If we assume bearings in the rotation stages are the entire cause, then a shift of  $h$  in the balls causes a tilt  $h/R$  of the rotation stage.

At the bearing, a shift of 10–60 nm accounts for the residual. The preload in the bearings probably makes the residual so small.

Table 1: Fit of image position to  $d(\theta) = A \cos(\theta + \phi) + B$  for three flexure runs. The conversion from pixels to an angle at the mirror assumes the flexure is entirely due to the tilt of the mirror. For f/12 run 2, the residual in parenthesis is the residual with the fit from run 1 removed.

	f/12, run 1		f/12, run 2		f/21		
	x	y	x	y	x	y	
$A$	$-0.16 \pm 0.01$	$1.76 \pm 0.03$	$-0.16 \pm 0.02$	$1.77 \pm 0.04$	$0.01 \pm 0.01$	$-2.67 \pm 0.07$	pixel
in sky	$-13 \pm 1$	$141 \pm 3$			$0.5 \pm 0.4$	$-107 \pm 3$	mas
at mirror	$-2.5 \pm 0.2$	$27.8 \pm 0.5$			$0.1 \pm 0.1$	$-29.1 \pm 0.7$	$\mu$ rad
$\phi$	$12 \pm 5$	$-11.4 \pm 1.3$	$38 \pm 8$	$-5.9 \pm 1.4$	$-2 \pm 50$	$45 \pm 1.3$	deg
residual	0.03	0.10	0.05 (0.06)	0.10 (0.15)	0.03	0.15	pixel
in sky	2.5	8	4 (4)	8 (12)	1	6	mas
at mirror	0.5	1.5			0.3	1.6	$\mu$ rad
at bearing	20	60			11	60	nm

<sup>2</sup>Baker, D., & Loh, E., 2005, “Acceptance Test of the Remanufactured PRS110 Rotation Stage.”

### 3 Reproducibility of Flexure

If reproducible, flexure can be eliminated on the telescope by varying the offset between the guide star and the object of interest. If flexure is not reproducible, then of course the image of a star will be elongated. Here we measured flexure with the f/12 channel a second time to test reproducibility.

The second run (middle row of Figure 3) matches the first run (top row) reasonably well. The fit (Table 1) shows that the amplitudes agree, but the phases disagree by  $d\phi_y = (5 \pm 2)^\circ$ .

Can the fit from run 1 be used to correct run 2? After correcting with the fit from run 1, the residual of the image location in the y-direction of run 2 (the right center plot of Figure 3) is small. The RMS residual  $(\sigma_x, \sigma_y) = (0.06, 0.15)$  pixel (Table 1). There is some sinusoidal behavior in the residual, as is evident in the plot. After removing the sinusoidal, the RMS residual,  $(0.05, 0.10)$  pixel, is slightly smaller.

If the fit from run 1 is used to correct run 2, the residual in the sky  $(\sigma_x, \sigma_y) = (4, 12)$  mas, which is much smaller than the the diffraction width, 80 mas at  $\lambda 1600$  nm.

### 4 Reproducibility of the Mechanisms

Here we measure the reproducibility of the mechanisms. We measure the location of the image, move a mechanism, move it back, and remeasure the position of the image. For the mechanisms for the f/12 camera mirror and the f/21 collimating mirror, a tilt in the bearing moves the image. For the mask wheel mechanism and 2-eye, a shift in the bearing axis moves the image, and a tilt changes the focus.

For the f/21 collimator and f/12 camera mechanisms, the image moves more than a pixel between insertion of the mirrors. (See Figure 4 for the data and Table 2 for a summary.) The movement in the direction of symmetry is smaller than that in the other direction.

It is not unreasonable that the image moves more in the case where the rotation stage turns than when only the direction of gravity changes. In the former case, the contacts between the balls and the race does not change. In the latter case, the balls move in the race, and the contact points change. For the flexure test, where the balls do not move in the race, the irreproducible movement of the balls is 10–60 nm. For test of repeatability, where the balls move in the race, the irreproducible movement of the balls is 300–1500 nm. Therefore, if the balls must roll in the race, the positioning is worse by a factor of 30.

The reproducibility of the mechanism for the mask wheel is excellent. Positioning repeats to  $0.5 \mu\text{m}$  in the direction of rotation and  $3 \mu\text{m}$  in the perpendicular direction,

which translates to 0.06 of the diffraction width.

The reproducibility of the mechanism for 2-eye is better than 0.01 pixel or  $0.2\ \mu\text{m}$ , which is the error of the measurement.

---

This material is based upon work supported by Michigan State University, the SOAR Telescope Consortium, the National Council for Scientific and Technological Development of Brazil (CNPq), the State of São Paulo Research Foundation (FAPESP), and the National Science Foundation under Grant No. 0242794. Any opinions, findings, and conclusions or recommendations expressed in this material are those of the author(s) and do not necessarily reflect the views of the National Science Foundation.

Table 2: Reproducibility of the mechanisms expressed as the standard deviation of all measurements. The conversion from pixels to an angle assumes the flexure is entirely due to the tilt of a mirror.

	f/12 Cam		f/21 Col		Mask		2 Eye		
	x	y	x	y	x	y	x	y	
at detector	0.5	1.7	0.7	3.7	0.02	0.13	0.01	0.01	pixel
in sky	40	140	30	150	0.8	5	0.4	0.4	mas
at optic	7	27	8	41					$\mu\text{rad}$
at bearing	300	1000	300	1500	500	3100	200	200	nm

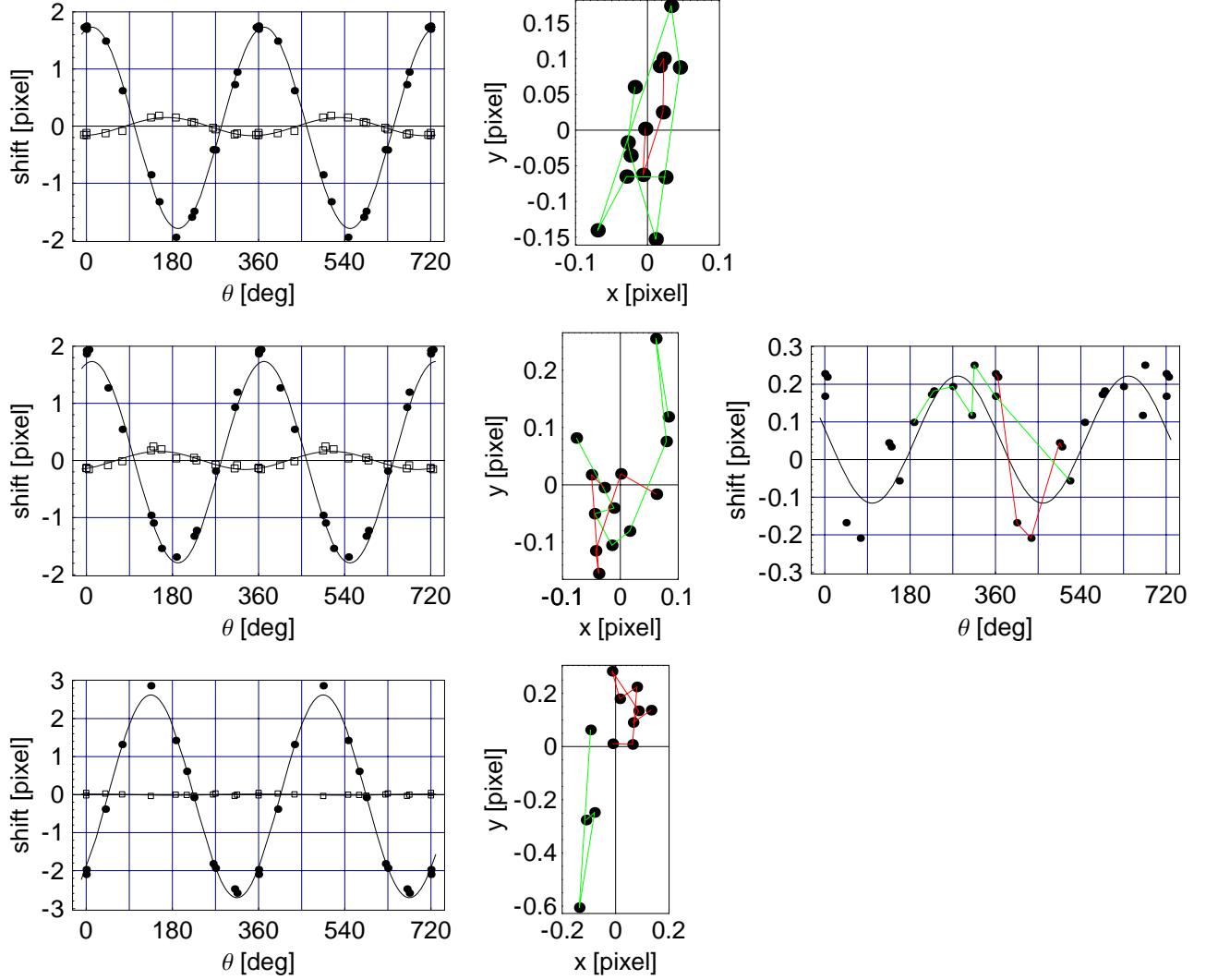


Figure 3: Left column: Shift of the image of a pinhole vs. orientation of the instrument. The shift in the x-direction, the direction of symmetry, is shown with rectangles; the shift in the y-direction is shown with dots. Run 1 for f/12 is on the top row; f/12 run 2 is on the middle row; f/21 channel is on the bottom. The data taken on different days have been shifted. The second column is the residual without a day-dependent shift. A red line connects points taken on the first day; the green line connects points taken on the second day. The plot on the far right shows the y-residual of the second f/12 run with the fit for the first f/12 run removed.

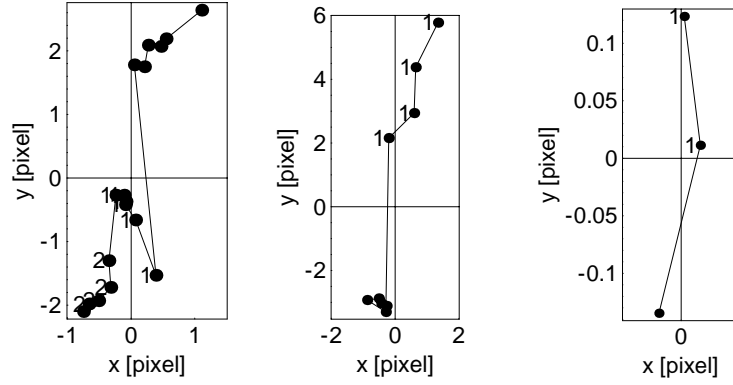


Figure 4: Image position after moving the mechanisms for the f/21 collimator (left), f/12 camera (center), and mask wheel (right). The mirror is moved out of the beam and back between each image, or the mask is turned  $90^\circ$  and back. The orientation of the instrument is  $135^\circ$  for points labelled “1,”  $-175^\circ$  for points labeled “2,” and  $0^\circ$  for unlabeled points. The instrument is symmetrical in the x-direction.